Available online at www.sciencedirect.com
ScienceDirect
C. R. Physique 9 (2008) 31–40
COMPTES RENDUS PHYSIQUE
http://france.elsevier.com/direct/COMREN/

New concepts for nanophotonics and nano-electronics

Metamaterials for optical and radio communications

Boubacar Kante, Abdelwaheb Ourir, Shah Nawaz Burokur, Frédérique Gadot, André de Lustrac *

Institut d'électronique fondamentale, université Paris-Sud, UMR 8622 – CNRS, 91405 Orsay cedex, France

Available online 11 February 2008

Abstract

We present here two examples of metamaterials for applications in the telecoms domain. The first concerns the realization of an ultra compact directive electronically reconfigurable antenna. The second deals with an infrared left-handed metamaterial working under normal incidence. For the first application, we use a composite phase varying metamaterial. An adjustable resonance radiating frequency between 7.9 and 8.2 GHz is obtained and a drastic enhancement in the directivity of the antenna is observed for a cavity thickness as small as $\lambda/75$ (0.5 mm!). Concerning the second application we present simulations and measurements of a metamaterial made of gold wires and C-shaped nanostructures on silicon at infrared wavelengths. Both plasmonic resonances occur at 1.7 and 4.2 μm, corresponding to a simultaneously negative permittivity and permeability. A simplified version of this metamaterial is realized in the microwave domain. This new metamaterial is characterized and the left-handed behavior is experimentally demonstrated. ***To cite this article: B. Kante et al., C. R. Physique 9 (2008).***

Résumé

Métamatériaux pour des applications optiques et télécoms. Nous présentons ici deux exemples de métamatériaux pour des applications dans le domaine des télécoms. Le premier concerne la réalisation d'une antenne directive ultra-compacte reconfigurable électroniquement utilisant une surface partiellement réfléchissante (PRS) réalisée à l'aide d'un métamatériau composite. Le second traite du fonctionnement d'un métamatériau gaucher infrarouge en incidence normale. Dans la première application, nous utilisons cette surface partiellement réfléchissante pour réaliser une antenne à cavité résonnante à 8 GHz. Le métamatériau considéré a une phase variable contrôlée à l'aide de composants électroniques actifs et est utilisé pour la conception d'une antenne reconfigurable de type Fabry–Perot. Une résonance réglable entre 7,9 et 8,2 GHz est obtenue et une amélioration importante de la directivité de l'antenne est également observée pour une épaisseur de cavité aussi petite que $\lambda/75$ (0,5 mm !). En ce qui concerne la deuxième application, nous présentons des simulations et des mesures effectuées sur un métamatériau fait de fils d'or et de nanostructures en forme de C, déposés sur un substrat de silicium aux longueurs d'onde infrarouges. Les deux résonances plasmoniques se produisent à 1,7 et à 4,2 μm, correspondant à une permittivité et une perméabilité simultanément négatives. Une version simplifiée de ce métamatériau destiné à la réalisation de superlentille en micro-onde est également proposée. Ce nouveau métamatériau est réalisé et caractérisé et son comportement gaucher est expérimentalement démontré. ***Pour citer cet article : B. Kante et al., C. R. Physique 9 (2008).***

Keywords: Metamaterial; Antenna; Varactor; Left-handed material; Plasmonic; Infrared metamaterial; Negative index

* Corresponding author.
E-mail address: andre.delustrac@ief.u-psud.fr (A. de Lustrac).

1631-0705/$ – see front matter
doi:10.1016/j.crhy.2007.10.004

Mots-clés : Métamatériau ; Antenne ; Varacteur ; Matériau à indice de réfraction négatif ; Plasmonique ; Métamatériau pour l'infra-rouge ; Indice de réfraction négatif

1. Ultra-compact directive electronically reconfigurable metamaterial antenna

1.1. Introduction

The half wavelength restriction of a Fabry–Perot cavity antenna can be reduced to respectively a quarter wavelength [1] and a tenth wavelength by making use of a metamaterial-based resonant cavity in order to design compact directive electromagnetic sources based on a single radiating antenna [2]. The principle is based on the use of a Partially Reflective Surface (PRS) with a frequency dependent reflection phase as a transmitting window. This PRS surface is made of a capacitive and an inductive grid and our group has lately further reduced the cavity thickness up to $\lambda/60$ for applications to ultra-thin directive antennas [3,4]. In [5], we have also shown the possibility of obtaining a passive steerable directive antenna using a novel 1-D composite metamaterial with a locally variable reflection and transmission phase. In this present work, we present the modeling and characterization of a resonant cavity for an electronically reconfigurable antenna near 8 GHz using an active phase varying metamaterial. The cavity is composed of a Perfect Electric Conductor (PEC) surface and of a composite metamaterial acting as the PRS with a tunable reflection and transmission phase. The cavity resonance is presently shown to occur for a cavity thickness as small as 0.5 mm ($\lambda/75$). This resonance radiating frequency is adjustable between 7.9 and 8.2 GHz. Furthermore, a drastic enhancement of the antenna directivity is obtained.

1.2. Design and characterization of the electronically tunable phase metamaterial

The cavity considered here is composed of the patch antenna's PEC ground plane and the PRS reflector placed at a distance h above the antenna (Fig. 1(a)). The PRS reflector consists of a periodic array of copper strips mechanically etched on each face of a 1.4 mm thick FR3-epoxy ($\varepsilon_r = 3.9$ and $\tan\delta = 0.0197$) substrate as shown in Fig. 1(b). The upper array where the strips are oriented parallel to the electric field $\boldsymbol{E}$ of the antenna plays the role of the inductive grid, whereas the lower array where the strips are oriented parallel to the magnetic field $\boldsymbol{H}$ acts as the capacitive grid. Instead of applying a linear variation of the gap spacing g in order to create a locally variable phase as in [4], we now use active components to make the phase of the PRS shift in frequency. Varactors are thus incorporated into the capacitive grid between two adjacent metallic strips (Fig. 1(b)) and depending on the applied bias voltage, the phase of the PRS varies with frequency. A prototype of the PRS is designed and fabricated where all the gaps present the same capacitance according to the bias voltage applied.

To do so, 8×8 unit cells are used and the overall dimensions of the prototypes are $60 \times 60 \times 1.4$ mm^3. The variable capacitive grid of the tunable phase PRS used for this work consists of a lattice of metallic strips with varactors connected each 6 mm ($s = 6$ mm) between two adjacent strips. This distance is chosen to be smaller than the wavelength. The width of the strips and the spacing between two strips of the capacitive grid are respectively $w = 1$ mm and $g = 2$ mm (Fig. 1(b)). RF inductances are used in the microstrip circuit in order to prevent high frequency signals going to the DC system. For the inductive grid, the width of the strips and the spacing between two strips are respectively $w_1 = 2$ mm and $g_1 = 4$ mm. Note that the inductive grid is not made tunable. By changing the bias voltage of the varactors of the PRS, the capacitance of the metamaterial will also vary. As a consequence, the phases of the reflection and transmission coefficients also vary as has been observed in [4]. This behavior is illustrated by the measurement results of the reflection coefficient phase shown in Fig. 2. The measurements are performed in an anechoic chamber using two horn antennas working in the 2–18 GHz frequency band and a 8722ES network analyzer as described in [3]. From Fig. 2, we can note that the variation of the bias voltage accounts for the shift of the resonance frequency. An increase in the bias voltage leads to a decrease in the value of the capacitance of the metamaterial, and finally a shift of the resonance towards higher frequencies. This phase shift is very important since it will help to tune the resonance frequency of the cavity antenna. Fig. 2(b) depicts the variation of the transmission of the PRS, function of the bias voltage V. Around 8 GHz the transmission increases with this bias voltage, and so the PRS is less and less reflective.

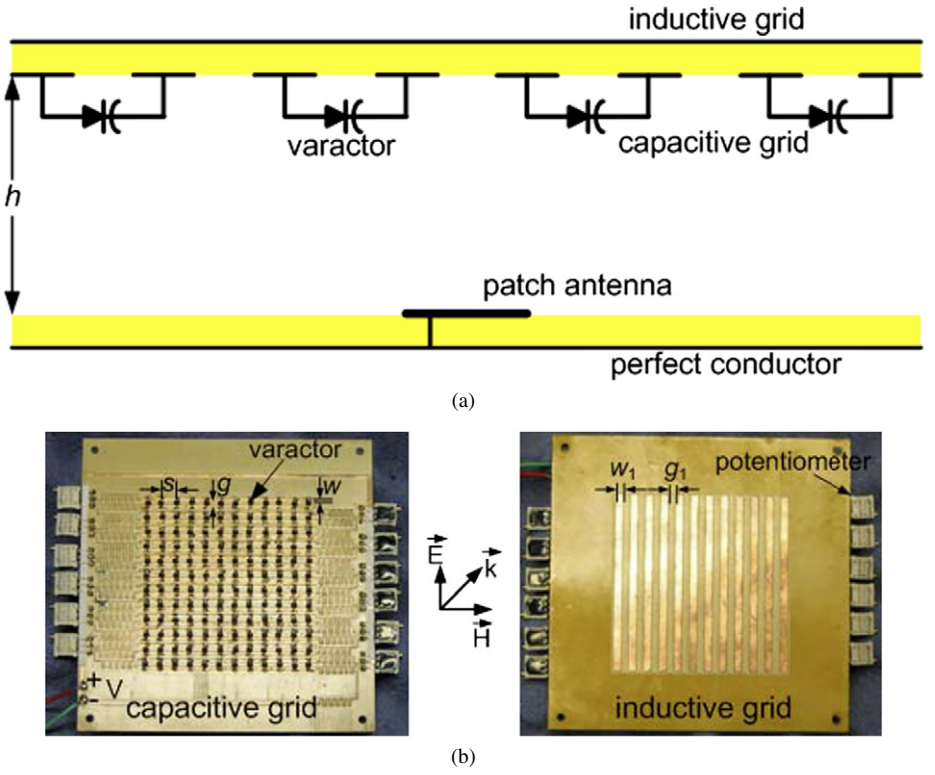

Fig. 1. (a) Schematic view of the cavity composed of a PEC and a electronically phase-varying PRS; (b) photographs of both sides of the composite metamaterial, showing the capacitive grid with varactors and the inductive grid.

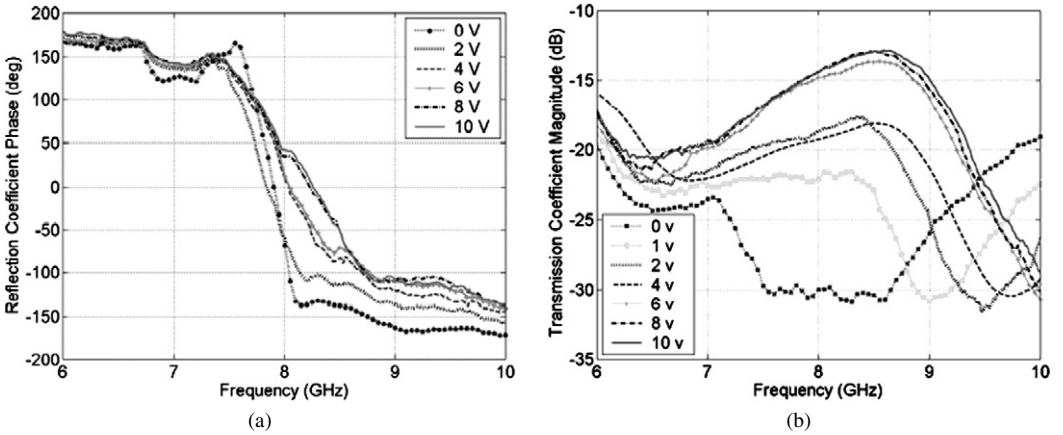

Fig. 2. (a) Reflection coefficient phase of the PRS with the bias voltage V of the varactors. A shift towards high frequencies and a decrease of the slope of the phase variation around 8 GHz are noted when V increases; (b) transmission of the PRS versus the varactor bias.

1.3. Tunable resonant frequency cavity antenna

A prototype of the sub-wavelength cavity has been fabricated. The PRS studied above is placed at a distance $h = 0.5$ mm above the feeding source which is a rectangular patch antenna with dimensions 9×9 mm^2. This patch antenna alone has a resonance frequency of 8.1 GHz. The resonance frequency of the proposed cavity, which depends on the phase of the reflection coefficient of the PRS and also on the cavity height h, is found to be in the vicinity of 8 GHz for the different bias voltages applied. Fig. 3(a) shows the matching of the cavity antenna with different bias voltage of the varactors. Two important observations can be made and are illustrated in this figure. Firstly, a shift

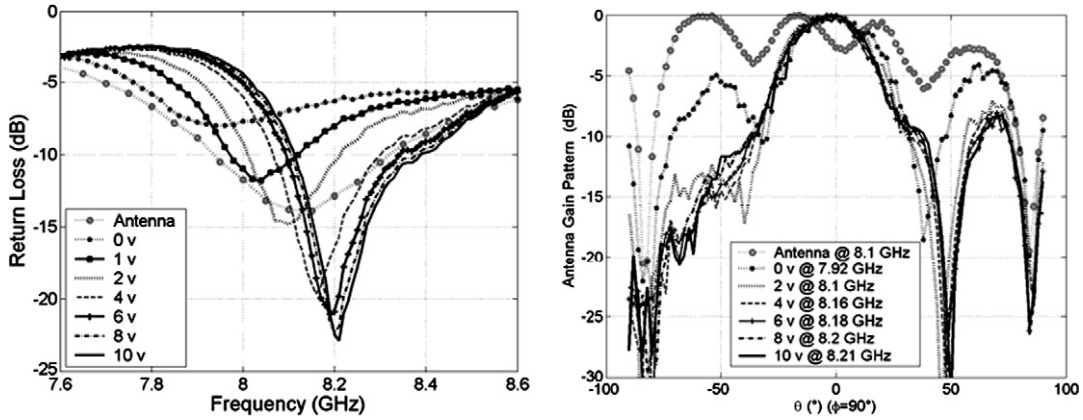

(a) (b)

Fig. 3. (a) Measured return losses of the antenna when the bias V of the varactors increases; (b) measured antenna gain pattern in the $\boldsymbol{E}$-plane ($\varphi = 90°$) at the resonance frequency when the bias voltage V increases.

towards high frequencies of the cavity resonance is noted when the bias voltage varies from 0 to 10 V, as for the reflection phase response. This is due to the decrease in the capacitance of the PRS. Moreover, it can be observed that the dip of the resonance increases when the bias voltage is tuned from 0 to 10 V, indicating an enhancement of the matching of the cavity. This enhancement is explained by the fact that the cavity antenna is better and better matched for the thickness $h = 0.5$ mm fixed when the bias voltage varies from 0 to 10 V. If we change the thickness h of the cavity, we obtain a better matching at another frequency since the resonance frequency depends on the reflection phase of the PRS as well as the cavity thickness h as shown in the relation given by Eq. (1) for the resonance condition:

$$h = (\phi_{\mathrm{PRS}} + \phi_{\mathrm{r}})\frac{\lambda}{4\pi} \pm N\frac{\lambda}{2} \tag{1}$$

where ϕ_{PRS} and ϕ_{r} are the reflection phase of respectively the PRS reflector and of the surface near the antenna (PEC), and N is the integer denoting the electromagnetic mode order of the cavity. Here $N = 0$ and h may be very small if the sum $(\phi_{\mathrm{PRS}} + \phi_{\mathrm{r}})$ is close to zero. As $\phi_{\mathrm{r}} \approx 180°$, ϕ_{PRS} must be near to $-180°$ to obtain a small value of h. If we consider Fig. 2(a), this is obtained for frequencies higher than the resonance frequency. Measurements of the radiation patterns of the reconfigurable cavity antenna are done in the anechoic chamber and are presented in Fig. 3(b). These patterns in the $\boldsymbol{E}$-plane ($\varphi = 90°$) are plotted for the case of the microstrip patch antenna alone and for the cavity antenna at different frequencies corresponding to the best matching obtained when the bias voltage is changed. When the capacitance of the PRS changes by a variation of the bias voltage of the varactors, a better directivity is obtained for the metamaterial-based cavity antenna compared to the case of the antenna alone.

A -3 dB beamwidth of 45° is thus observed for the cavity antenna instead of more than 100° for the microstrip antenna alone. However, we can note from that a secondary lobe with quite a high magnitude appears on the radiation pattern when the bias of the varactors is 0 V. This high magnitude may be probably due to the weak transmission (-30 dB in Fig. 2(b)) and the small side dimensions of the PRS (60×60 mm^2). When the transmission of the PRS is weak, the wave emitted by the antenna is reflected by the PRS and it is guided between the PRS and the metallic ground reflector and emitted at the limits of the cavity. This explains the secondary lobes at null bias. When the bias is increased, the transmission of the PRS increases and the side lobes decrease rapidly and we obtain a more directive antenna. An optimization of this cavity should reduce the level of this secondary lobe and enhance the performances. The directivity of the cavity antenna can be calculated using the following expression: $D = 41\,253/(\theta_1 \times \theta_2)$ where θ_1 and θ_2 are respectively the half-power widths (in degrees) for the $\boldsymbol{H}$-plane and $\boldsymbol{E}$-plane patterns. In our case, the directivity is found to be approximately equal to 14.85 dB for bias voltage range (2–10 V).

1.4. Summary

Sub-wavelength metamaterial-based planar surfaces are used for applications to ultra-compact highly directive cavity antennas. An electronically tunable Partially Reflective Surface composed of a composite phase varying

metamaterial, made of a periodic capacitive grid and an inductive one. The capacitive grid is made tunable by the incorporation of active electronic components (varactors). This composite metamaterial is proposed for the design of a frequency reconfigurable cavity antenna. The resonance frequency is determined by the height h of the cavity and the reflection phase of the PRS. A shift of this resonance frequency is noted when the bias voltage of the varactors increases. This shift corresponds to the decrease of the elementary cell capacitance of the PRS. A better matching of the antenna and a drastic enhancement of the directivity is also observed when the bias voltage increases.

2. Asymmetrical left-handed metamaterial in microwave and infrared regimes under normal to plane incidence

2.1. Introduction

V. Veselago has theoretically studied materials with a simultaneously negative permeability and permittivity in 1968 [6]. In 1999, J.B. Pendry [7] demonstrated the possibility to design such materials artificially and the first prototype fabricated by Smith et al. [8] involved considerable efforts from the scientific community to understand the physical properties of such structures. These structures can effectively lead to the design of superlenses with very high resolution going well beyond the Rayleigh limit [9]. Several techniques have been proposed for the realization of these metamaterials. The first one, initiated by Smith, consists in alternating Split Ring Resonators (SRR) and continuous metallic strips. The second one consists in using bi-layer structures composed of discontinuous metallic wires as proposed by Zhang et al. and Shalaev et al. [10,11]. In this paper, we first present the near infrared prototype fabricated at the Institut d'électronique fondamentale (IEF) together with the simulation and measurement results. Then, we compare this metamaterial with a bi-layer one used in the microwave regime by Ozbay et al. [12], that we propose to transform towards an asymmetrical mono-layer structure. This monolayer structure coincides with our fabricated structure when the lateral legs of the resonators are removed. It shows several advantages compared to the published structures. It works under normal to plane incidence and is relatively simple to fabricate in the infrared. Its fabrication in the visible region can then be considered.

2.2. Negative refractive index metamaterial in the near infra-red regime at normal incidence

Metamaterials are sub-wavelength artificial structures where the dimensions are very small compared to the working wavelength. These dimensions are typically of the order of $\lambda/10$ where λ is the wavelength propagating in the material. This condition allows one to consider the metamaterial as an effective one and also to describe the behavior of the wave propagating in it. Recently, we have fabricated a metamaterial made of gold SRR and continuous metallic wires on silicon, presenting plasmonic resonances at around 6 and 2 μm.

Fig. 4(a) shows a Scanning Electronic Microscope (SEM) image of the fabricated prototype. The periodicity of the structure's unit cell is about 570 nm and the wires have a 20 nm thickness and 50 nm width (Fig. 4(b)). The dimensions of the SRR are 250 nm × 300 nm with a gap of 160 nm.

2.3. Design, simulation and experimental results

Using the commercial code Ansoft's *HFSS*, a bi-periodic structure considered infinite in the lateral directions has been simulated at normal incidence. Fig. 5(a) shows the simulated results for two polarizations considered, depending on whether $\boldsymbol{E}$ is parallel or perpendicular to the gap of the resonator. These results are compared to measurements made with a Fourier Transform Infra-Red spectrometer (FTIR) on the fabricated prototype shown in Fig. 5(b). A good agreement is observed. We should note that for the simulation of the metallic parts with *HFSS*, a Drude model has been used to represent the permittivity of gold. This model is given by Eq. (2):

$$\varepsilon(\omega) = 1 - \frac{\omega_{\mathrm{p}}^2}{\omega(\omega + \mathrm{i}\omega_{\mathrm{c}})} \tag{2}$$

where $\omega_{\mathrm{p}} = 2 \times 10^{16}\ \mathrm{s}^{-1}$ and $\omega_{\mathrm{c}} = 6.478 \times 10^{13}\ \mathrm{s}^{-1}$ are respectively the plasma and collision angular frequency of gold [13]. As in this reference, the value of the plasma frequency is adjusted to fit the simulation results to the measurements. The value of the collision frequency ω_{c} is the same as in the reference [13]. In both simulation and

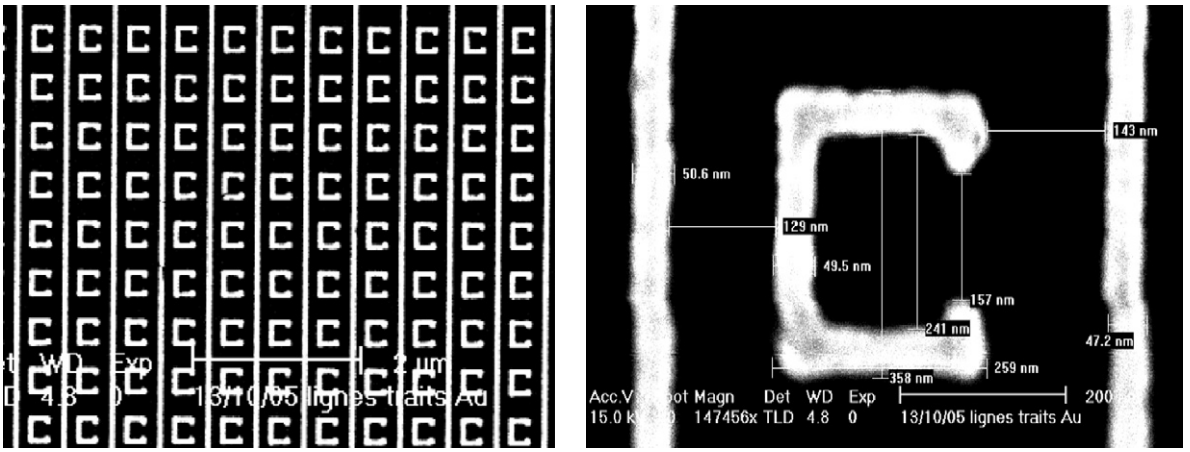

(a) (b)

Fig. 4. (a) Scanning Electronic Microscope (SEM) image of the metamaterial; (b) unit cell showing the different dimension of the SRR and the wire.

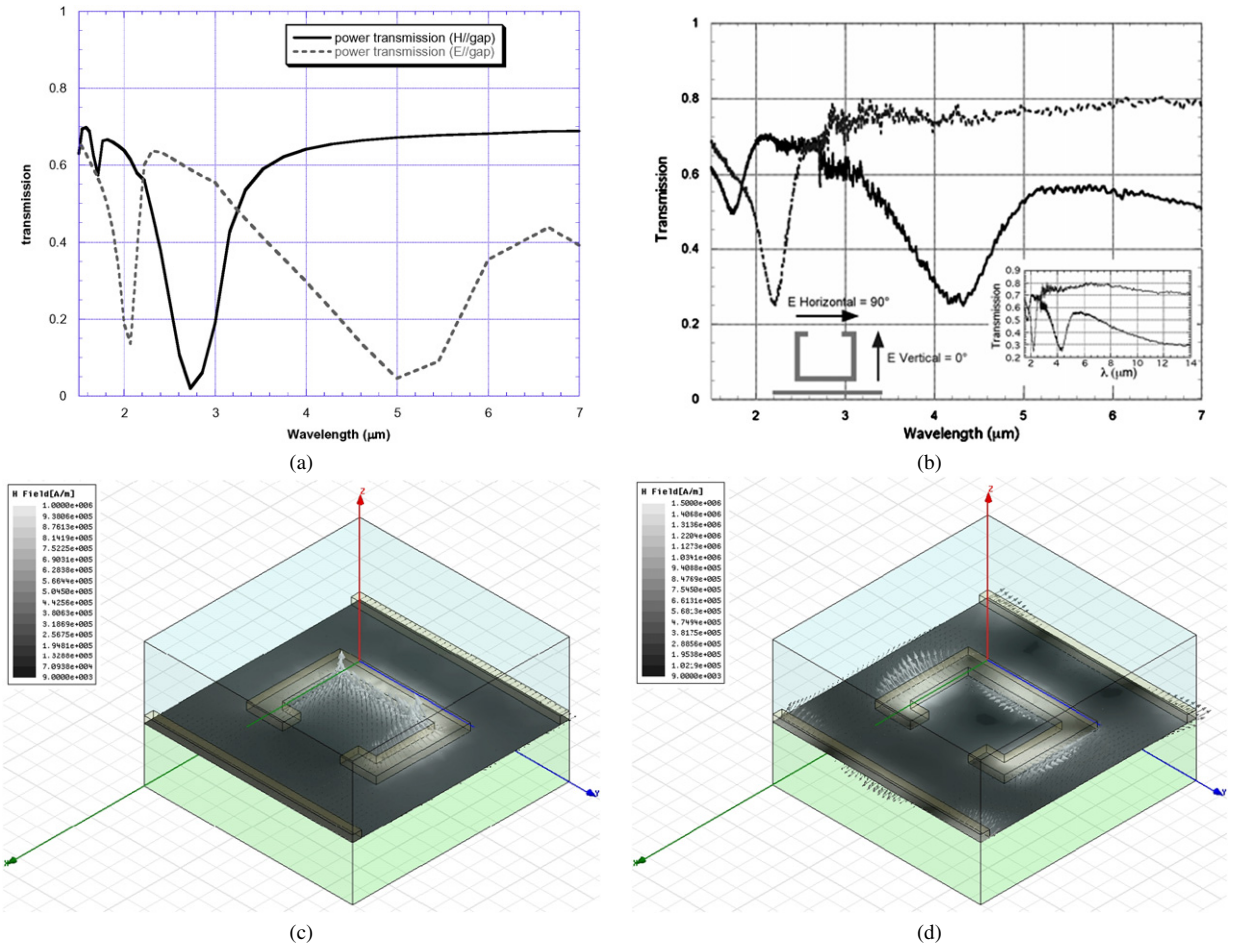

(a) (b)

(c) (d)

Fig. 5. (a) Simulated transmission response; (b) measured transmission response of the metamaterial at normal incidence. The black and grey lines represent respectively the case when $\boldsymbol{E}$ is parallel and perpendicular to the gaps of the resonator. The insert in (b) shows the measured transmission on a wider band (1.5 to 14 μm). (c) Magnetic field $\boldsymbol{H}$ in the plane of the SRR at the lower resonance frequency when $\boldsymbol{E}$ is parallel to the gap; (d) magnetic field at the higher resonance frequency.

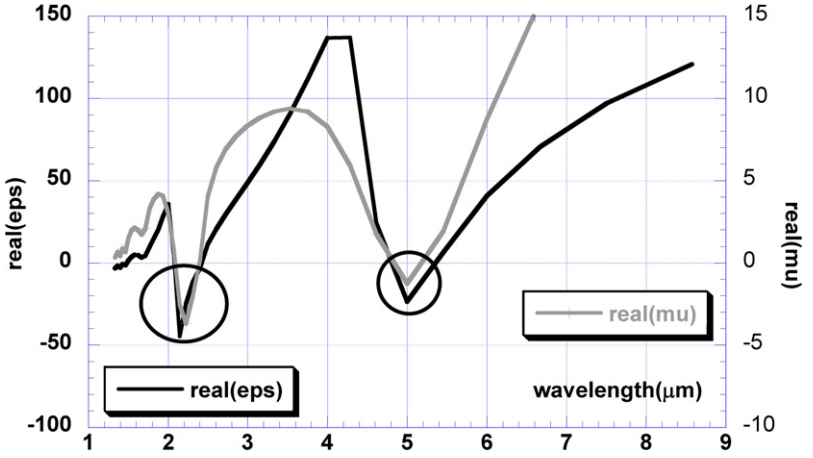

Fig. 6. Real parts of the calculated permeability and permittivity.

measurements, we can observe two resonances respectively at 1.7 and 4.2 μm in measurements and at 2 and 5.1 μm in simulation when $\boldsymbol{E}$ is parallel to the gap.

The shift in frequency between the measured and simulated results is probably due to the values taken for the Drude model parameters ω_p and ω_c concerning the gold permittivity. Rockstuhl et al. identify both resonances as plasmonic resonances [14]. When $\boldsymbol{E}$ is parallel to the gap, the lower frequency resonance corresponds to an electromagnetic mode of the SRR only (Fig. 5(c)). The higher resonance corresponds to a coupling mode between the metallic wire and the parallel side of the SRR (Fig. 5(d)). Fig. 5(c) shows the magnetic field $\boldsymbol{H}$ in the plane of the SRR at the lower resonance frequency when $\boldsymbol{E}$ is parallel to the gap. The plasmonic mode concerns only the SRR. Fig. 5(d) shows the magnetic field at the higher resonance frequency. The coupling between the metallic wire and the side of the SRR parallel to the wire is clearly seen. It is also seen that resonance frequency is determined by the size of the side of the SRR parallel to the electric field. Here this side length is 300 nm and if we consider the silicon substrate of the SRR, this gives a wavelength of $\lambda = 2 \times 300.10^{-9} \times \sqrt{11.6} = 2$ μm, very close to the measured value. The resonance occurs when the half-wavelength coincides with the optical length of the horizontal SRR arm. When $\boldsymbol{E}$ is perpendicular to the gap of the resonator, only one plasmonic resonance is observed at 2.8 μm in simulations and 2.2 μm in measurements. This resonance corresponds to a plasmonic mode of the lateral legs of the SRR parallel to the electric field [14].

The effective parameters of the metamaterial have also been calculated from the results of the simulations, using the Nicholson and Ross approach [15], and are presented in Fig. 6. The effective permeability and permittivity are negative in the vicinity of the plasmonic resonances, i.e., at 2.2 and 5 μm (60 and 140 THz).

2.4. Asymmetric left-handed metamaterial for the microwave and infra-red regimes

The preceding structure is asymmetrical and Ozbay et al. have recently proposed a symmetrical bi-layer metamaterial [16] in the microwave regime, around 14 GHz, made of continuous metallic wires and cut-wires (Fig. 7(a)). The continuous wires allow it to have a negative permittivity for frequencies below plasma frequency ω_p of the lattice [17]. The bi-layer material made of cut-wires is modeled as an L–C circuit exhibiting a negative permeability around its resonance frequency ω_r at normal incidence. If this resonance frequency is lower than the plasma frequency ω_p, the material will present a left handed behavior around ω_r. This structure can be transformed by removing the metallic layer on one face and one of the continuous wires on the other face of the substrate to obtain an asymmetrical structure. Figs. 7(a)–(c) illustrate the transformation of the structure step by step towards our proposed one (Fig. 7(c)). A transposition in the infrared regime is then undertaken (Figs. 7(d)–(f)). The U shape resonators legs lengths have been progressively diminished till completely removed. It appears that the last structure of Figs. 7(c) and (f) have similar unit cells though the first one operates in the microwave regime and the second one in the near infrared regime. We have simulated, fabricated and characterized the structure of Fig. 7(c) in the microwave domain using the finite element based software *HFSS* from Ansoft. The dimensions are the same as in Ref. [16].

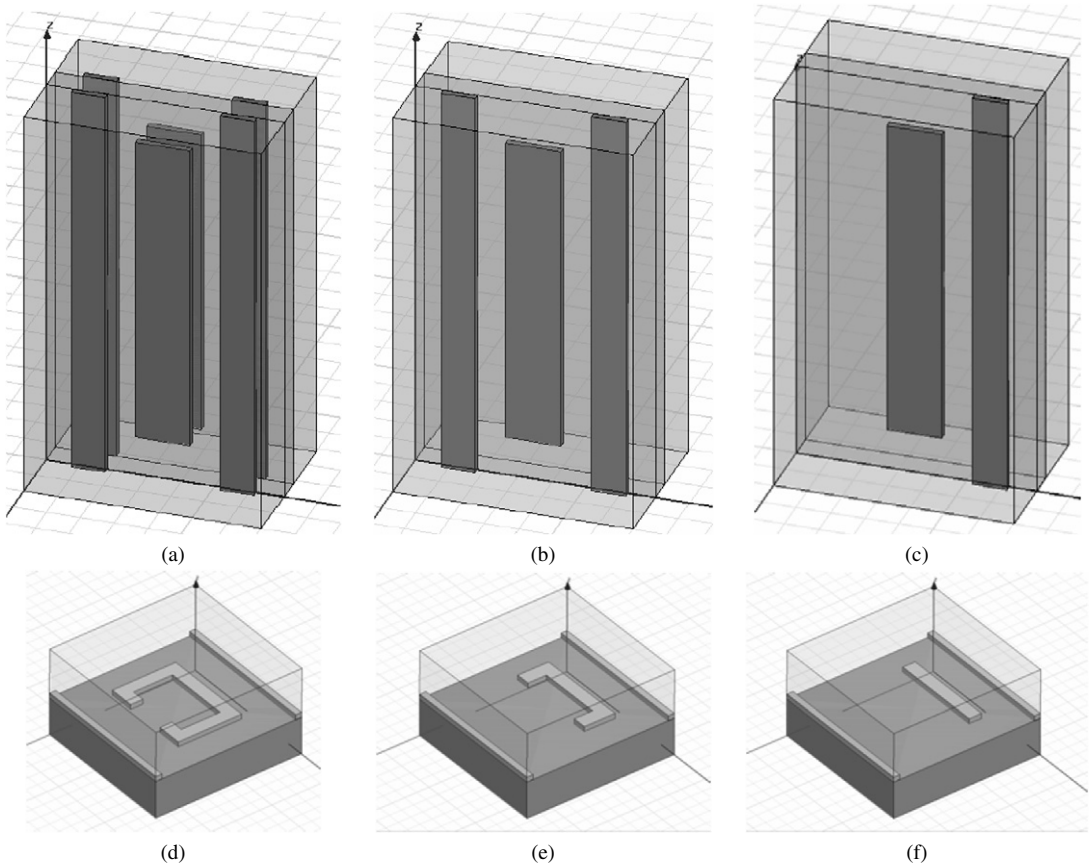

Fig. 7. The three structures derived from that proposed by Ozbay in the microwave regime ((a)–(c)); and the three structures proposed in infra-red ((d)–(f)).

Ozbay et al. have demonstrated theoretically and experimentally for the structure of Fig. 7(a) that one of the fundamental properties of left-handed materials is the phase shift when stacking an increasing number of materials layers in the direction of the wave propagation [16]. The phase decreases algebraically with an increasing number of layers instead of increasing, as in a right-handed material. This test is used to identify a left-handed behavior using one, two and three layers of the metamaterial. The electric field $\boldsymbol{E}$ is polarized parallel to the continuous wires for normal to plane propagation. The structure is assumed to extend to infinity in the lateral directions. Fig. 8 shows the results of the simulation and of the measurements of the structure of Fig. 7(c) in the microwave domain. In Fig. 8(a) the measured transmission and reflection of one layer under normal to plane incidence (black and grey solid lines) are compared to the simulated ones (black and grey dashed lines). In Fig. 8(b) we have compared the evolution of the measured transmission phase for one, two and three layers. In the range 12–15 GHz the phase increases negatively with the number of layers. This evolution may correspond to a left-handed behavior of the material. To verify this proposition, we have also calculated from the measurement results the effective permittivity and permeability. Fig. 9 shows the results of these calculations. Fig. 9(a) depicts the real values of the permittivity and of the permeability deduced from the measurements for one layer. Fig. 9(b) corresponds to the same quantities for three stacked layers. In this figure the real parts of the permittivity and the permeability are simultaneously negative for frequencies in the range 15–16 GHz corresponding to the left-handed behavior of the material [6].

However, the frequency range where the real parts of the permittivity and of the permeability are negative is smaller than the range where the phase evolves negatively with the number of layers. This demonstrates that the criterion of the negative phase evolution is necessary but not sufficient to justify the left-handed behavior of the material.

This structure is interesting to transpose in infrared because of its simplicity. The manufacture of this structure is under way.

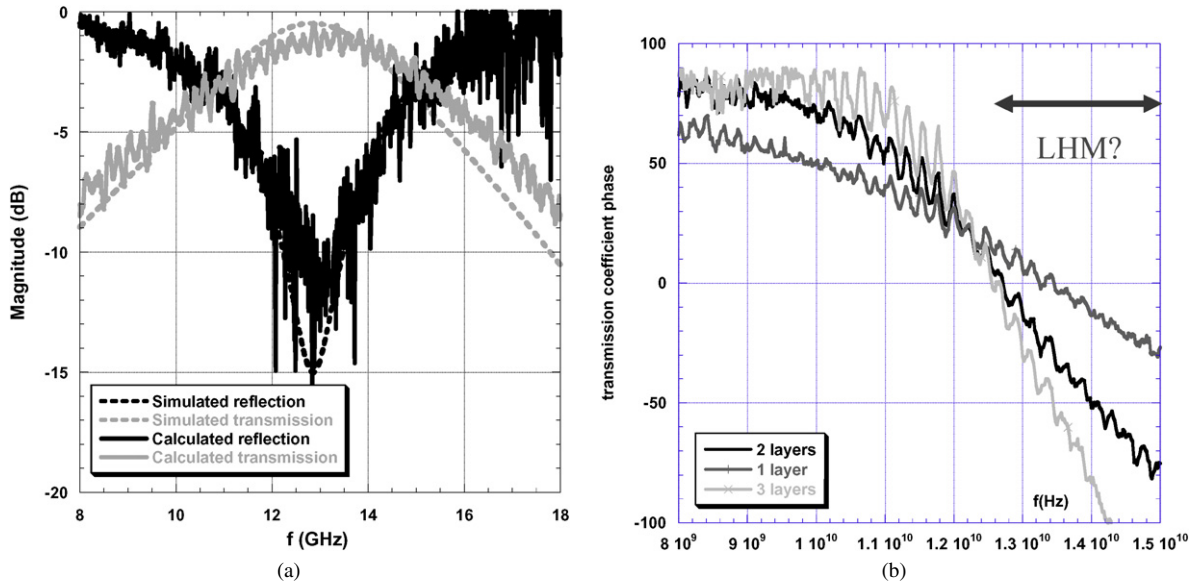

(a) (b)

Fig. 8. (a) Measured transmission and reflection (black and grey solid lines) compared to the simulated ones (black and grey dashed lines). (b) Evolution of the measured transmission phase for one, two and three layers. For frequencies above 12 GHz, the phase increases negatively with the number of layers.

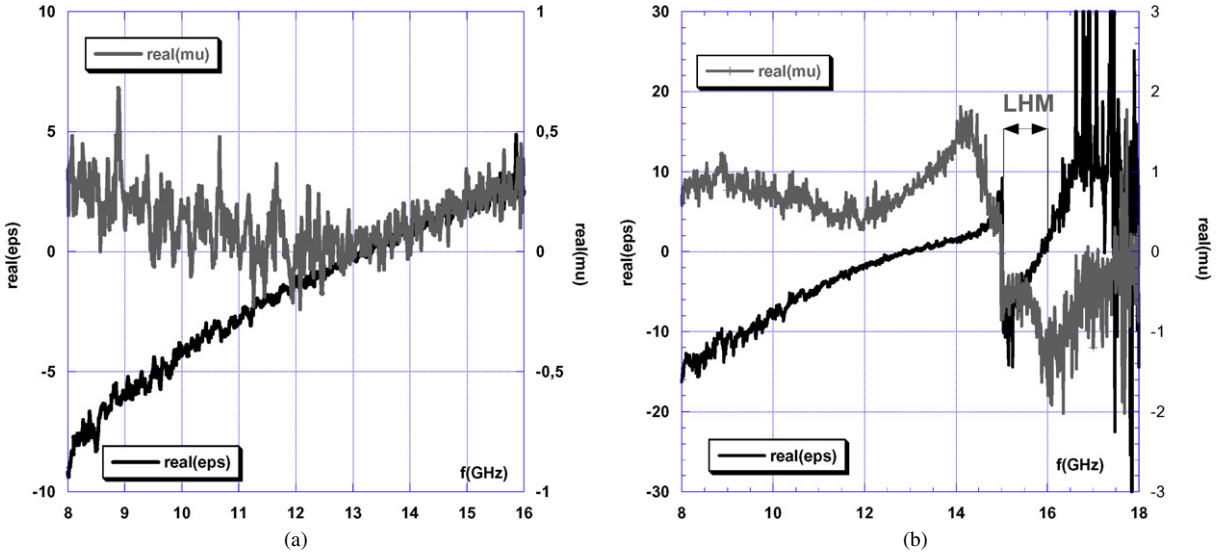

(a) (b)

Fig. 9. Real values of the permittivity and of the permeability for (a) one and (b) three layers. In (b) the left-handed behavior corresponds to the frequency range 15–16 GHz.

2.5. *Summary*

A left-handed metamaterial working in the near infrared regime (2 μm), made of gold continuous wire and SRR (Split Ring Resonators), has been fabricated and characterized at normal incidence. The structure exhibits a left-handed behavior when the electric field is parallel to the gap of the SRR. Transforming this structure towards an asymmetrical one by removing the legs of the U shape resonator allows it to preserve the left-handed behavior. This coincides with the transformation of the bi-layer symmetric structure proposed by Ozbay et al. when this one is transformed into a monolayer asymmetrical structure. This asymmetrical structure has a broad frequency band where

the left-handed behavior occurs. The simplicity of this structure allows its integration in complex devices like super lens for applications in the microwave and infrared domains.

3. General conclusion

In this paper we have proposed two types of metamaterials for applications in the microwave and infrared domains. The first deals with the development of an ultra-compact directive antenna for the telecoms in X band. The metamaterial used in this antenna is a composite made of a capacitive and inductive surfaces. Its main property is the control of the reflection phase, function of the frequency through the geometrical parameters of the two surfaces. The second concerns mainly the design and the characterization of a new type of left-handed material suitable for imaging applications in the microwave and infrared domains. A first prototype, made of gold wires and C-shaped resonators on silicon, is realized and characterized at infrared frequencies. This device shows plasmonic resonances around 1.7 and 4.2 μm. The simulation of the material shows a left-handed behavior at these resonances. A second metamaterial with a simplified design is proposed simultaneously in the microwave and infrared domains. It has been fabricated and characterized at microwave frequencies, showing a broad frequency range where the left-handed behavior occurs. The fabrication of this metamaterial at infrared and visible frequencies is under way. Both examples show the richness of the metamaterial concept and the number of their potential developments.

References

[1] A.P. Feresidis, G. Goussetis, S. Wang, J.C. Vardaxoglou, Artificial magnetic conductor surfaces and their application to low-profile high-gain planar antennas, IEEE Trans. Antennas Propag. 53 (1) (2005) 209–215.
[2] L. Zhou, H. Li, Y. Qin, Z. Wei, C.T. Chan, Directive emissions from subwavelength metamaterial-based cavities, Appl. Phys. Lett. 86 (2005) 101101-1–101101-3.
[3] A. Ourir, A. de Lustrac, J.-M. Lourtioz, All-metamaterial-based sub-wavelength cavities ($\lambda/60$) for ultrathin directive antennas, Appl. Phys. Lett. 88 (2006) 084103-1–084103-3.
[4] A. Ourir, A. de Lustrac, J.-M. Lourtioz, Optimization of metamaterial based subwavelength cavities for ultracompact directive antennas, Microw. Opt. Technol. Lett. 48 (12) (2006) 2573–2577.
[5] A. Ourir, S.N. Burokur, A. de Lustrac, Phase-varying metamaterial for compact steerable directive antennas, Electron. Lett. 43 (9) (2007) 493–494.
[6] V.G. Veselago, The electrodynamics of substances with simultaneously negative values of permittivity and permeability, Sov. Phys. Usp. 10 (1968) 509–514.
[7] J.B. Pendry, A.J. Holden, W.J. Stewart, Magnetism from conductors and enhanced nonlinear phenomena, IEEE Trans. Microw. Theory Tech. 47 (11) (1999) 2075–2084.
[8] D.R. Smith, W.J. Padilla, D.C. Vier, S.C. Nemat-Nasser, S. Schultz, Composite medium with simultaneously negative permeability and permittivity, Phys. Rev. Lett. 84 (18) (2000) 4184–4187.
[9] J.B. Pendry, Negative refraction makes a perfect lens, Phys. Rev. Lett. 85 (18) (2000) 3966–3969.
[10] S. Zhang, W. Fan, N.C. Panoiu, K.J. Malloy, R.M. Osgood, S.R.J. Brueck, Demonstration of near-infrared negative-index metamaterials, Phys. Rev. Lett. 95 (2005) 137404-1–137404-4.
[11] V.M. Shalaev, W. Cai, U.K. Chettiar, H.-K. Yuan, A.K. Sarychev, V.P. Drachev, A.V. Kildishev, Negative index of refraction in optical metamaterials, Opt. Lett. 30 (24) (2005) 3356–3358.
[12] K. Guven, M.D. Caliskan, E. Ozbay, Experimental observation of left-handed transmission in a bilayer metamaterial under normal-to-plane propagation, Opt. Exp. 14 (19) (2006) 8685–8693.
[13] S. Linden, C. Enkrich, M. Wegener, J. Zhou, T. Koschny, C.M. Soukoulis, Magnetic response of metamaterials at 100 terahertz, Science 306 (2004) 1351–1353.
[14] C. Rockstuhl, F. Lederer, On the reinterpretation of resonances in split-ring-resonators at normal incidence, Opt. Exp. 14 (19) (2006) 8827–8836.
[15] A.M. Nicholson, G.F. Ross, Measurement of the intrinsic properties of materials by time-domain techniques, IEEE Trans. Instrum. Meas. IM-19 (4) (1970) 377–382.
[16] K. Aydin, K. Guven, C.M. Soukoulis, E. Ozbay, Observation of negative refraction and negative phase velocity in left-handed metamaterials, Appl. Phys. Lett. 86 (2005) 124102-1–124102-3.
[17] J.B. Pendry, A.J. Holden, D.J. Robbins, W.J. Stewart, Low frequency plasmons in thin-wire structure, J. Phys. Condens. Matter 10 (22) (1998) 4785–4809.